ELSEVIER

Neurochemistry International 36 (2000) 397–409

NEUROCHEMISTRY International

www.elsevier.com/locate/neuint

Glial cells and volume transmission in the CNS

Eva Syková*, Alexandr Chvátal

Department of Neuroscience, 2nd Medical Faculty, Charles University and Institute of Experimental Medicine, Academy of Sciences of the Czech Republic, Vídeňská 1083, 142 20, Prague 4, Czech Republic

Received 22 April 1999; received in revised form 17 August 1999; accepted 19 August 1999

Abstract

Although synaptic transmission is an important means of communication between neurons, neurons themselves and neurons and glia also communicate by extrasynaptic "volume" transmission, which is mediated by diffusion in the extracellular space (ECS). The ECS of the central nervous system (CNS) is the microenvironment of neurons and glial cells. The composition and size of ECS change dynamically during neuronal activity as well as during pathological states. Following their release, a number of neuroactive substances, including ions, mediators, metabolites and neurotransmitters, diffuse via the ECS to targets distant from their release sites. Glial cells affect the composition and volume of the ECS and therefore also extracellular diffusion, particularly during development, aging and pathological states such as ischemia, injury, X-irradiation, gliosis, demyelination and often in grafted tissue. Recent studies also indicate that diffusion in the ECS is affected by ECS volume inhomogeneities, which are the result of a more compacted space in certain regions, e.g. in the vicinity of oligodendrocytes. Besides glial cells, the extracellular matrix also changes ECS geometry and forms diffusion barriers, which may also result in diffusion anisotropy. Glial cells therefore play an important role in extrasynaptic transmission, for example in functions such as vigilance, sleep, depression, chronic pain, LTP, LTD, memory formation and other plastic changes in the CNS. In turn, ECS diffusion parameters affect neuron–glia communication, ionic homeostasis and movement and/or accumulation of neuroactive substances in the brain.

1. Extracellular space as a communication channel between cells

The extracellular space (ECS) of the central nervous system (CNS) is the microenvironment of the neurons and glial cells. It was shown using a number of different techniques, e.g., electron microscopy that preserves the ECS, radiotracers and ion diffusion methods, that the average ECS volume is 15–25% of the total adult brain volume (for review see Nicholson and Syková, 1998). The composition of the ECS changes dynamically during neuronal activity and in pathological states. A number of neuroactive substances are released into the ECS, e.g., ions, transmitters, peptides, neurohormones and metabolites, which diffuse via the ECS to their targets located on nerve as well as glial cells, distant from the release sites (for review see Syková, 1997). In contrast to neurons, which communicate by synaptic transmission, glial cells do not form synapses and interact with neurons by the diffusion of ions and other neuroactive substances through the ECS. The ECS thus serves as an important communication channel between cellular elements in the CNS. The extrasynaptic movement by diffusion through the ECS is called "extrasynaptic transmission", or "diffusion transmission", or "volume transmission", i.e. substances move through the *volume* of the ECS (Agnati et al., 1995; Nicholson and Syková, 1998; Syková, 1997; Zoli et al., 1999). Diffusion parameters of the ECS and their changes during neuronal activity, development, aging and many pathological states, substantially affect the movement of neuroactive substances in the ECS and may thus affect neuronal signaling and neuron–glia communication. Extrasynaptic trans-

* Corresponding author. Tel.: +420-2-475-2204; fax: +420-2-475-2783

E-mail address: sykova@biomed.cas.cz (E. Syková).

0197-0186/00/$ - see front matter
PII: S0197-0186(99)00131-X

mission in the brain may also be involved in the modulation of "massive" information processing such as vigilance, sleep, depression, chronic pain, LTP, LTD, memory formation and other plastic changes in the CNS (Syková, 1997). Glial cells play an important role in extrasynaptic transmission by affecting ECS composition and volume and by forming diffusion barriers. These diffusion barriers may be formed by fine glial and neuronal processes as well as by adhesion molecules and molecules of the extracellular matrix.

2. Role of glial cells in ionic homeostasis

The ionic composition of the ECS in the brain closely matches the composition of the cerebrospinal fluid. For example, in mammals it is: 141 mM Na^+, 124 mM Cl^-, 3 mM K^+, 121 mM HCO_3^-, 1.2 mM Ca^{2+} and about 2.5 mM Mg^{2+}. The introduction of ion-sensitive microelectrodes (ISM) with a liquid ion-exchanger for K^+ by Walker (1971), and later for other ions (e.g. Cl^-, H^+, Ca^{2+}), made it possible to follow the dynamic extracellular and intracellular ionic changes during neuronal activity in the normally functioning CNS as well as during pathological states (for reviews see Syková, 1983, 1992, 1997).

Ionic and volume homeostasis in the CNS is maintained by a variety of mechanisms present in neurons as well as in glial cells. It was shown in a number of studies in vivo as well as in vitro that changes in extracellular K^+ concentration ($[K^+]_e$), alkaline and acid shifts in pH_e and a decrease in extracellular Ca^{2+} concentration ($[Ca^{2+}]_e$) accompany neuronal activity in different brain regions (for review see Syková, 1983, 1992; Chesler, 1990). For example, in the immediate vicinity of individual neurons in the mesencephalic reticular formation (MRF) of the rat, a structure with a high spontaneous activity level, dynamic changes in $[K^+]_e$ have been described. During a burst of spontaneous action potentials, K^+ accumulates in the close vicinity of a firing cell and $[K^+]_e$ steadily increases by as much as 0.1 mM (Fig. 1A; Syková et al., 1974). Most frequently, neuronal activity results not only in an increase in $[K^+]_e$, but also in a decrease in $[Ca^{2+}]_e$ and in a rapid extracellular alkaline shift, followed by a slower but longer-lasting acid shift (Syková, 1992). After sustained adequate stimulation (Fig. 1B) of the afferent input or after repetitive electrical stimulation

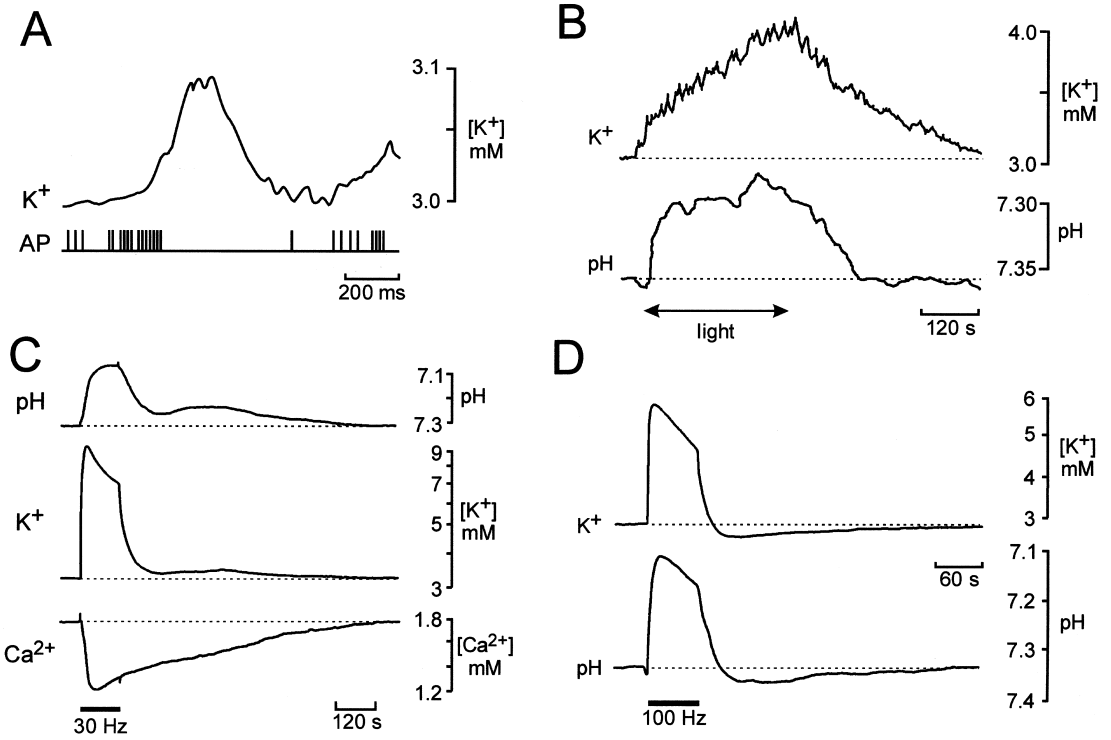

Fig. 1. Changes of K^+, pH and Ca^{2+} in the extracellular space of the nervous tissue during spontaneous activity and stimulation. A: The neuronal action potential bursts (AP) are accompanied by an increase in $[K^+]_e$ in the rat mesencephalic reticular formation. B: Increase in $[K^+]_e$ and acid shift in pH_e evoked in ectostriatum of the chick by light stimulation of the contralateral eye. C: $[K^+]_e$, pH_e and $[Ca^{2+}]_e$ changes in the dorsal horns of the isolated frog spinal cord evoked by the repetitive supramaximal stimulation of dorsal root VIII. D: Stimulation-evoked $[K^+]_e$ and pH_e changes in the spinal dorsal horn of adult rat. The change in pH_e was biphasic: first a small and fast "initial" alkaline shift occurred, which was followed by a dominating acid shift. Note the poststimulation undershoots in both, $[K^+]_e$ and pH_e.

(Fig. 1C, D), the ionic transients reach a certain steady state, the so-called "ceiling" level. The K^+ ceiling level found in the adult mammalian cortex is about 7 mM K^+ (Heinemann and Lux, 1977) and in the mammalian spinal cord 6–8 mM K^+ (Kříž et al., 1974; Syková and Svoboda, 1990). The alkaline shifts in mammalian cortex, cerebellum or spinal cord do not exceed 0.02 pH units, while the acid shifts are about 0.2 pH units (for reviews see Chesler, 1990; Deitmer and Rose, 1996; Syková, 1992). When stimulation is continued, a gradual decrease of both transients, $[K^+]_e$ and pH_e, occurs after the ceiling levels are reached due to homeostatic mechanisms in neurons and glial cells (Fig. 1C, D). The redistribution of activity-related ionic changes is mediated, at least partially, by the Na^+,K^+-ATPase transport mechanism, which is located in neurons as well as in glial cells. It was shown that after stimulation, a transient decrease in $[K^+]_e$ occurs below the original baseline, the so-called poststimulation K^+-undershoot, which is blocked by ouabain or during hypoxia (Heinemann and Lux, 1977; Kříž et al., 1975). Besides the Na^+/K^+ pump activity, K^+ homeostasis in the ECS is also maintained by three other mechanisms located in glial cells: (1) K^+ spatial buffering; (2) KCl uptake; and (3) Ca^{2+}-activated K^+ channels.

It was shown in a number of studies that pH changes in the ECS are caused by neurons as well as by glial cells. There is now convincing evidence for the neuronal origin of extracellular alkaline shifts and the glial origin of activity-related acid shifts (Jendelová and Syková, 1991; Syková et al., 1992). During early postnatal development, when glial cell function is incomplete, activity-related pH_e and $[K^+]_e$ changes are substantially different from those observed in adult animals with completed gliogenesis and glial cell function. In the neonatal rat spinal cord, stimulation-evoked changes in $[K^+]_e$ are much larger than in the adult animal (Fig. 2A, B; Jendelová and Syková, 1991). In newborn rats, alkaline shifts dominate in the ECS, since the acid shifts generated by glia are small. At postnatal day 10, when gliogenesis in rat spinal cord gray matter peaks, the K^+ ceiling level decreases and stimulation evokes acid shifts in the range of 0.1–0.2 pH units, which are preceded by scarcely discernible alkaline shifts, also observed in adult rats (Fig. 2A, B). Stimulation-evoked alkaline shifts are, in addition, abolished by the blockage of synaptic transmission by Mn^{2+} or Mg^{2+}, while acid shifts are unaffected (Syková et al., 1992). Similar results were observed in chicks, in which light stimulation or the application of the bitter tasting substance methylantranilate (MeA) resulted in alkaline shifts in pH_e in hyperstriatum ventrale of the brain in 3-day-old chicks. It was not until 10 days after hatching that an acid shift replaced the alkaline (Fig. 2C), suggesting

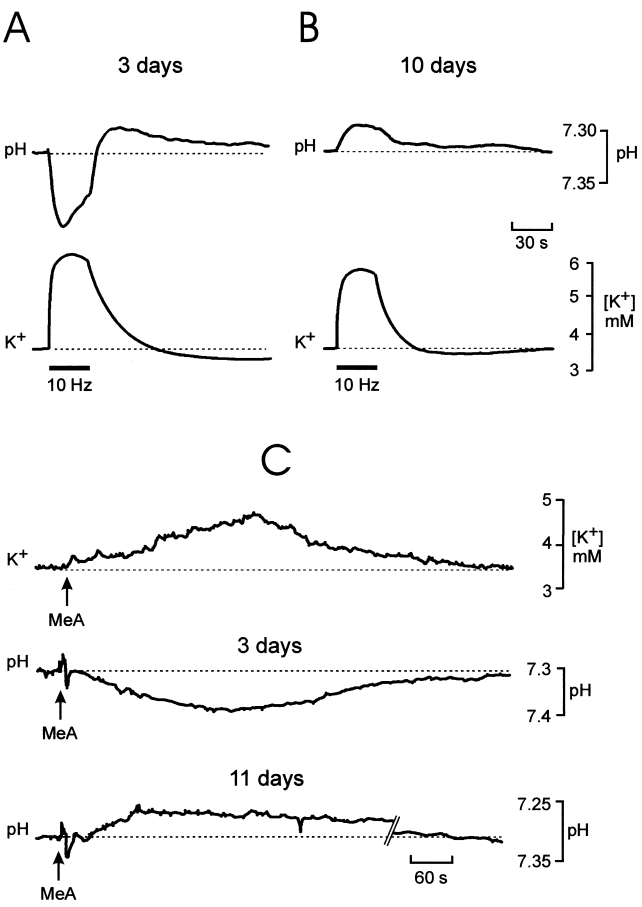

Fig. 2. Stimulation-evoked $[K^+]_e$ and pH_e changes during early postnatal development. A: Repetitive electrical repetitive stimulation of the dorsal root in 3-day-old rats was accompanied by an alkaline shift and by an increase in $[K^+]_e$. When stimulation was discontinued a poststimulation acid shift of smaller amplitude appeared, which was accompanied by a K^+-undershoot. B: In the 10-day-old rat the $[K^+]_e$ increase was smaller and was accompanied by an extracellular acid shift. C: The effect of taste aversant methylantranilate (MeA) placed on the tongue of anesthetized chicks on $[K^+]_e$ and pH_e recorded in the hyperstriatum ventrale at postnatal days 3 and 11. In 3-day-old chicks MeA evoked an alkaline shift, while in 11-day-old chicks only an acid shift was detected.

that glial cells are functionally mature at this stage (Ng et al., 1992). Alkaline shifts resulting from neuronal activity are depressed, e.g., by the application of the GABA antagonist picrotoxin and by glutamate receptor antagonists and channel blockers such as MK801 (non-competitive NMDA receptor antagonist and channel blocker) and CNQX (competitive AMPA/kainate receptor antagonist) (Jendelová et al., 1994; Syková et al., 1992). Glial cells play an important role in buffering activity-related alkaline changes in extracellular pH.

Some of the membrane transport processes regulating intra- and extracellular pH, such as Na^+/H^+ exchange and $Na^+/H^+/Cl^-/HCO_3^-$ cotransport, are

present in both neurons and glia, while others are specific either for neurons (e.g., H^+ channels, H^+ or HCO_3^- permeability of the ionic channels opened by GABA or glutamate) or for glia (e.g., the voltage-dependent Na^+–HCO_3^- cotransport and lactate extrusion). The glial cell membrane is also readily permeable to CO_2, which reacts with H_2O to form carbonic acid, which in turn quickly dissociates into water and protons. This reaction is enhanced by the catalytic action of the enzyme carbonic anhydrase, which is almost exclusively present in glial cells. Some of the membrane transport mechanisms result in alkaline shifts in pH_e (acid loaders), while others result in acid shifts in pH_e (acid extruders), but it is evident that acid loaders are dominant in neurons, while acid extruders are dominant in glia (Chesler, 1990; Deitmer and Rose, 1996; Syková, 1992). Extracellular acid shifts are, therefore, a consequence of activity-related $[K^+]_e$ increase. K^+-induced glial depolarization results in an alkaline shift in glial pH_I, which leads to the stimulation of classical acid extrusion systems in glial cells. Membrane mechanisms responsible for the transport of ions across the cell membrane are always accompanied by the movement of water, thus affecting the cell volume and the size of the ECS (Fig. 3).

3. Diffusion parameters of the ECS

The diffusion of substances in a free medium, such as water or diluted agar, is described by Fick's laws. In contrast to a free medium, diffusion in the ECS of the nervous tissue is hindered by the size of the extracellular clefts, the presence of membranes, fine neuronal and glial processes, macromolecules of the extracellular matrix and charged molecules, and also by cellular uptake. To take these factors into account, it was necessary to modify Fick's original diffusion equations (see Nicholson and Phillips, 1981; Nicholson and Syková, 1998). First, diffusion in the CNS is constrained by the restricted volume of the tissue available for the diffusing particles, i.e., by the extracellular space volume fraction (α), which is a dimensionless quantity and is defined as the ratio between the volume of the ECS and the total volume of the tissue. It is now evident that the ECS in adult brain amounts to about 20% of the total brain volume, i.e., $\alpha = 0.2$. Second, the free diffusion coefficient (D) in the brain is reduced by the tortuosity factor (λ). ECS tortuosity is defined as $\lambda = (D/ADC)^{0.5}$, where D is a free diffusion coefficient and ADC is the apparent diffusion coefficient in the brain. As a result of tortuosity, D is reduced to an apparent diffusion coefficient $ADC = D/\lambda^2$. Thus, any substance diffusing in the ECS is hindered by membrane obstructions, glycoproteins, macromolecules of the ECM, charged molecules and fine neuronal and glial cell processes. Third, substances released into the ECS are transported across membranes by non-specific concentration-dependent uptake (k'). In many cases however, these substances are transported by energy-dependent uptake systems that obey non-linear kinetics (Nicholson, 1995). When these three factors (α, λ and k') are incorporated into Fick's law, diffusion in the CNS is described fairly satisfactorily (Nicholson and Philips, 1981).

The real-time iontophoretic method is used to determine ECS diffusion parameters and their dynamic changes in nervous tissue in vitro as well as in vivo (Nicholson and Syková, 1998; Syková, 1997). Ion-sensitive microelectrodes are used to measure the diffusion of ions to which the cell membranes are relatively impermeable, e.g. TEA^+, TMA^+ or choline. These substances are injected into the nervous tissue by pressure or by iontophoresis from an electrode aligned

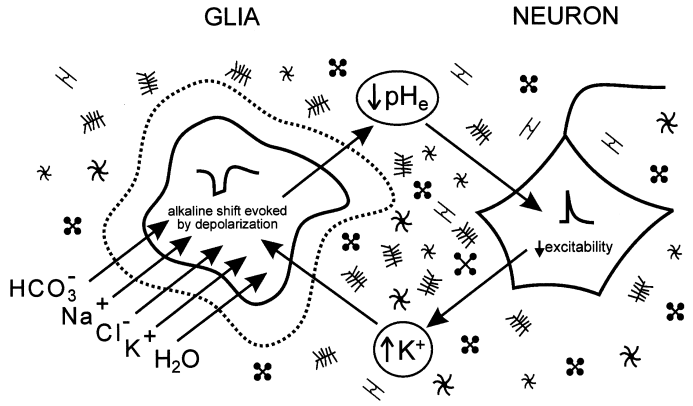

Fig. 3. Schematic of the mechanism of nonspecific feedback suppressing neuronal excitability. Active neurons release K^+, which accumulates in the ECS and depolarizes glial cells. This causes an alkaline shift in glial pH_i and an acid shift in pH_e. Extracellular acidosis further suppresses neuronal activity. Transmembrane ionic movements result in glial swelling, an ECS volume decrease and therefore in a greater accumulation of ions and neuroactive substances and crowding of molecules of the extracellular matrix in the ECS.

parallel to a double-barreled ISM at a fixed distance (Fig. 4). Usually, such an electrode array is made by gluing together a pressure or iontophoretic pipette and a TMA^+-sensitive ISM with a tip separation of 130–200 μm. In the case of iontophoretic application, the TMA^+ is released into the ECS by applying a current step of +100 nA with a duration of 40–80 s. The released TMA^+ is recorded with the TMA^+-ISM as a diffusion curve (Fig. 4), which is then transferred to a computer. Values of the ECS volume, *ADC*s, tortuosity and non-specific cellular uptake are extracted by a non-linear curve-fitting simplex algorithm applied on the diffusion curves.

By introducing the tortuosity factor into diffusion measurements in nervous tissue, it soon becames evident that diffusion is not uniform in all directions and is affected by the presence of diffusion barriers including neuronal and glial processes, myelin sheaths, macromolecules and molecules with fixed negative surface charges. This so-called anisotropic diffusion preferentially channels the movement of substances in the ECS in one direction, (e.g., along axons) and may, therefore, be responsible for a certain degree of specificity in volume transmission. Diffusion anisotropy was found in the CNS in the molecular and granular layer of the cerebellum (Rice et al., 1993), in the hippocampus (Mazel et al., 1998; Pérez-Pinzon et al., 1995) and in the auditory but not in the somatosensory cortex (Syková et al., 1999a), and a number of studies revealed that it is present in the myelinated white matter of corpus callosum or spinal cord (Fig. 4; Chvátal et al., 1997; Prokopová et al., 1997; Voříšek and Syková, 1997). It was shown that diffusion anisotropy in white matter increases during development. At first, diffusion in unmyelinated tissue is isotropic; it becomes more anisotropic as myelination progresses.

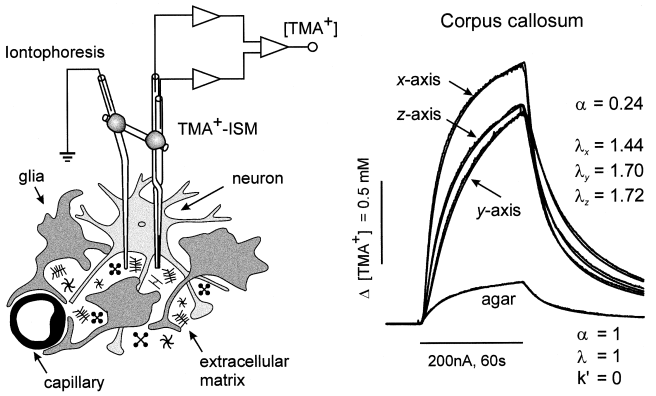

Fig. 4. Experimental set-up, TMA^+ diffusion curves and typical ECS diffusion parameters α (volume fraction) and λ (tortuosity) obtained in the white matter of the CNS (corpus callosum — CC). Left: Schema of the experimental arrangement. A TMA^+-selective double-barreled ion-selective microelectrode (ISM) was glued to a bent iontophoresis microelectrode. The separation between electrode tips was 130–200 μm. Right: Typical TMA^+ diffusion curves obtained in agar and in CC made in three orthogonal axes (*x, y* and *z*) showing anisotropic diffusion. The *x*-axis lies along the axons while the *y*- and *z*-axes lie across the fibers. All recordings are from the same animal at P21. The slower rise in the *z* than in the *y* direction and in the *y* than in the *x* direction indicates a higher tortuosity and more restricted diffusion. Actual ECS volume fraction α is about 0.2 and can be calculated only when measurements are done along the *x*-, *y*- and *z*-axes. Recordings were first made in agar, where by definition $\alpha = 1 = \lambda$ and $k' = 0$, and the electrode transport number (n) and diffusion coefficient of the TMA^+ (D) are extracted by curve fitting. Knowing n and D, the parameters α, λ, and k' were obtained in all three axes in CC. The shape and amplitude of the diffusion curves reflect the different apparent diffusion coefficients (*ADC*s), i.e. λ values, associated with each axis.

The other methods that are also used to study ECS volume and geometry, e.g., intrinsic optical signals (IOS), tissue resistance, integrative optical imaging (IOI) and nuclear magnetic resonance (NMR), are less comprehensive because they can measure only relative changes in the ECS diffusion parameters or only some of the three diffusion parameters (Andrew and MacVicar, 1994; Korf et al., 1988; Matsuoka and Hossmann, 1982; Nicholson and Tao, 1993; Van Harreveld et al., 1971). Integrative optical imaging is used to measure the *ADC*s of molecules tagged with fluorescent dye, while recordings of intrinsic optical signals, either light transmittance or light reflectance, are believed to reflect changes in the ECS volume; however, direct evidence is missing. On the other hand, diffusion-weighted NMR methods provide information only about the water diffusion coefficient (Benveniste et al., 1992; Latour et al., 1994; Norris et al., 1994; Van der Toorn et al., 1996), and the relationships between water diffusion maps and changes in cell volume and ECS diffusion parameters are still not understood.

4. Glial cells and ECS diffusion parameters

All transmembrane ionic shifts, e.g., K^+, Na^+, Ca^{2+} and H^+, and membrane transport mechanisms such as glutamate uptake, are followed by water movement, thus causing the shrinkage or swelling of neural cells including glia.

Neuroactive substances, ions and neurotransmitters released during neuronal activity or during pathological states into the ECS interact not only with the neuronal membranes at pre- or postsynaptic sites, but also with extrasynaptic receptors, including those on glial cells. Glial cells respond to such stimulation by the activation of ion channels, second messengers and intracellular metabolic pathways. Simultaneously, the cell volume of glial cells increases, including the swelling and rearrangement of their processes, thus causing dynamic variations in the ECS volume. Glial cells, in addition to their role in the maintenance of extracellular ionic homeostasis, may therefore influence extra-

cellular pathways for the diffusion of neuroactive substances. In the central nervous system, many pathological processes are accompanied by the loss of nerve cells or their processes, by astrogliosis, manifested as an increase in glial fibrillary acidic protein (GFAP) staining, by demyelination, and, in addition, by changes in the extracellular matrix. All these processes lead to changes in CNS architecture and may therefore affect the diffusion of neuroactive substances in the ECS. The mechanisms of the changes in ECS diffusion parameters were studied during both normal and pathological states such as cell swelling evoked by the application of high K^+ or osmotic stress, astrogliosis inducted by trauma (stab wound), gliogenesis blocked by early postnatal X-irradiation, gliosis in tissue grafts, demyelination (experimental autoimmune encephalomyelitis, EAE), degeneration and astrogliosis during aging.

4.1. Effect of high K^+ and osmotic stress

It was shown in a number of studies that astrocyte swelling is an early event in numerous pathological states accompanied by the elevation of $[K^+]_e$ and a decrease of extracellular osmolarity (Kimelberg, 1991; Kimelberg and Ransom, 1986; Kimelberg et al., 1992). It was also shown that in the isolated turtle cerebellum exposed to hypotonic medium, volume fraction decreased to 0.12, while in hypertonic medium it increased to as much as 0.60 (Križaj et al., 1996). In isolated spinal cords of 4–21-day-old rats, incubation in either 50 mM K^+ (Fig. 5A) or hypotonic solution (235 mmol/kg) resulted at first in a decrease of the ECS volume fraction and in an increase in tortuosity in gray as well as in white matter (Syková et al., 1999c). These changes were evoked by cell swelling, since the total water content (TW) in spinal cord was unchanged. The observed changes of ECS diffusion parameters were blocked in Cl^--free solution and were slowed down by furosemide and bumetanide. During a continuous 45 min application of high K^+ or hypotonic solution, ECS volume fraction and tortuosity started to return towards control values, apparently due to the shrinkage of previously swollen cells by regulatory volume decrease (Cserr et al., 1991; Gullans and Verbalis, 1993; Strange, 1992). This cell volume regulation was not effective in immature animals with less advanced gliogenesis, nor in tissue slices of brain or spinal cord, and was blocked by the application of the gliotoxin fluoroacetate, thus suggesting that most of the changes were caused by glial cell swelling. Diffusion in myelinated spinal cord white matter was anisotropic, i.e., more facilitated along fibers than across them. The increase in tortuosity measured across fibers was greater than that along fibers, reaching unusually high values above 2.4. The application of 50 mM K^+ or hypotonic solution for 45 min evoked astrogliosis, which persisted even when these solutions were replaced with physiological saline. As astrogliosis increased, a second permanent rise in tortuosity was observed, while the ECS volume fraction either returned to control values or even exceeded them. In spinal cord white matter, a persistent increase in tortuosity after the washout of high K^+ or hypotonic solution was also found, and, in addition, the typical diffusion anisotropy was diminished.

4.2. Diffusion parameters of the ECS in gliotic tissue

A stab wound of the rodent brain is a well-characterized and common model of reactive gliosis, which

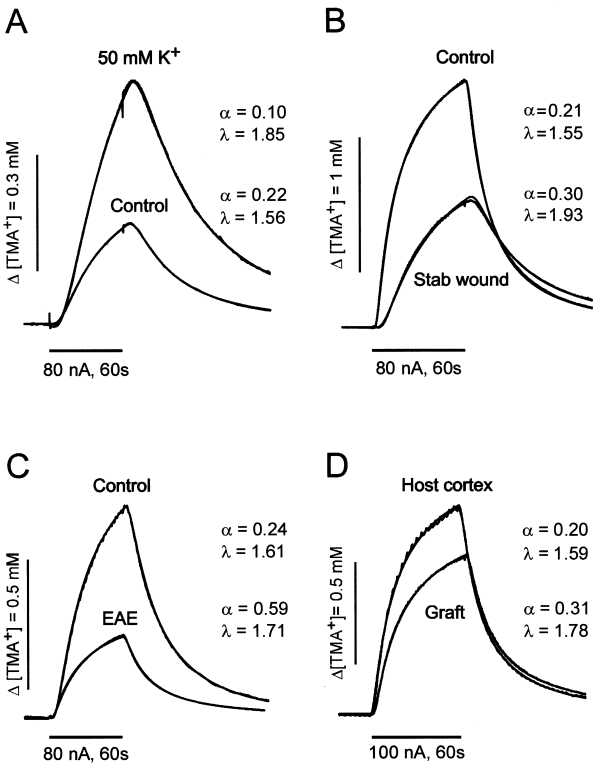

Fig. 5. TMA^+ diffusion curves under different experimental conditions. For each curve, the ECS diffusion parameters α (volume fraction) and λ (tortuosity) were extracted by appropriate non-linear curve fitting. Experimental and theoretical curves are superimposed in each case. For each figure the concentration scale is linear. A: Typical recordings in isolated rat spinal cord of a 13-day-old rat before (control) and during application of 50 mM K^+. Cellular, particularly glial, swelling results in an ECS volume decrease and a tortuosity increase. B: Typical recordings obtained in rat cortex (control). Values of α and λ are increased in the gliotic cortex around a stab wound. Note that the larger the curve, the smaller the value of α; a slower rise and decay indicate higher tortuosity. C: Representative recordings obtained in spinal cord segment L4 of a control and EAE Lewis rat as measured at a depth of 2200 μm from the dorsal surface. Note the dramatic increase in the ECS volume and the increased tortuosity during EAE. D: Typical recordings obtained in adult rat host cortex and in cortex-to-midbrain graft 135 days after transplantation at a depth of 700 μm from the brain surface.

can impose diffusion barriers in the CNS due to the hypertrophy of astrocytic processes and an increased production of extracellular matrix components (Hatten et al., 1991; Norton et al., 1992; Ridet et al., 1997). ECS diffusion parameters were therefore measured in the tissue surrounding a stab wound 3, 7, 21 and 35 days post-wounding (dpw) in the hemispheres ipsilateral and contralateral to the lesion (Fig. 5B; Roitbak and Syková, 1999). In the area 300–1000 μm around the wound, the ECS volume fraction increased at 3, 7 and 21 dpw by about 20%, but returned to control values at 35 dpw, while tortuosity increased at all four intervals, reaching a maximum at 7 dpw. Nonspecific TMA^+ uptake was lower than in the contralateral hemisphere at 7, 21 and 35 dpw. Measurements that were made at a greater distance from the wound (1500–2000 μm) revealed only an increase in tortuosity at 7 dpw. Immunostaining of the tissue sections for GFAP and chondroitin–sulphate proteoglycans (CSPG) after diffusion measurements revealed that the time course of changes in the ECS diffusion parameters closely correlated with increased staining for GFAP and CSPG. These experiments revealed that glial swelling and astrogliosis are associated with a long-term increase of diffusion barriers in the ECS, and can, therefore, lead to the impairment of the diffusion of neuroactive substances, extrasynaptic transmission and cell-to-cell communication in the CNS (Roitbak and Syková, 1999). Astrogliosis evoked by traumatic injury significantly affects the ECS diffusion properties, and both hypertrophied astrocytic processes as well as enhanced formation of extracellular matrix molecules may limit the diffusion of neuroactive molecules in the ECS.

4.3. Properties of the nervous tissue during development and after X-irradiation

During postnatal development diffusion parameters in the rat brain and spinal cord are different from those in adult rats (Lehmenkühler et al., 1993; Prokopová et al., 1997; Voříšek and Syková, 1997). The volume fraction is 50–100% larger and tortuosity lower than in adult rat. Volume fraction is decreasing during the entire postnatal life with the steepest decrease in early postnatal development. The larger ECS ($\alpha = 0.30$–0.45) in the first days of postnatal development in the rat can be attributed to incomplete neuronal migration, gliogenesis, angiogenesis and to the presence of large extracellular matrix proteoglycans, particularly hyaluronic acid, which due to the mutual repulsion of its highly negatively charged branches occupies a great deal of space and holds cells apart. The ensuing decrease in the ECS size could be explained by the disappearance of a significant part of the ECS matrix, neuronal migration and the development of dendritic trees, rapid myelination and the proliferation of glia.

The CNS during the early postnatal period is more sensitive to X-irradiation than is the adult nervous system, apparently due to the proliferative potential and increased radiation sensitivity of glial and vascular endothelial cells in the immature nervous system (Fike and Gobbel, 1991). It was shown in rat spinal cord that early postnatal X-irradiation is responsible for the impairment of gliogenesis and for a number of neurotoxic effects (Gilmore, 1964; Sims and Gilmore, 1992).

In experiments on the somatosensory neocortex and subcortical white matter of 1-day-old (P1) rats, X-irradiation at a single dose of 40 Gy resulted in radiation necrosis with typical early morphological changes in the tissue, namely cell death, DNA fragmentation, extensive neuronal loss, blood–brain–barrier (BBB) damage, activated macrophages, astrogliosis, an increase in extracellular fibronectin, and concomitant changes in all three diffusion parameters. The changes were observed as early as 48 h post-irradiation (at P2–P3) and persisted at P21 (Syková et al., 1996). Under normal conditions, the volume fraction of the ECS in the cortex is large in newborn rats, $\alpha = 0.35$–0.40, and diminishes with age (Lehmenkühler et al., 1993). X-irradiation at a single dose of 40 Gy blocked the normal pattern of volume fraction decrease during postnatal development and resulted in a significant increase in the ECS volume (Syková et al., 1996). At P4–P5, volume fraction in both cortex and corpus callosum increased to about 0.50. This increase persisted at 3 weeks after X-irradiation. Tortuosity and non-specific uptake significantly decreased at P2–P5; at P8–P9 they were not significantly different from those of control animals, and both significantly increased with astrogliosis at P10–P21. These data indicate that in chronic lesions, which occur 1–3 weeks after X-irradiation and/or in gliotic tissue, the volume fraction remains elevated, while tortuosity increases due to astrogliosis. Even when X-irradiation at a single dose of 20 Gy was used, resulting in relatively light neuronal damage and loss and BBB damage, it produced similar changes in diffusion parameters as those found with 40 Gy. Less pronounced but significant changes in diffusion parameters were also found in areas adjacent to the directly X-irradiated cortex of the ipsilateral hemisphere and in the contralateral hemisphere.

It is evident that the block of postnatal gliogenesis and the damage to neurons evoked by X-irradiation results in an even greater increase in the ECS volume fraction of nervous tissue than injury evoked by stab wound. Thus it can substantially contribute to impaired signal transmission, e.g. by diluting ions and neuroactive substances released from cells, and may thus play an important role not only in functional defi-

cits, but also in malfunctions during the developmental processes. Moreover, the increase in ECS volume and tortuosity in the X-irradiated cortex as well as in the contralateral hemisphere suggests that the diffusion of substances can be substantially changed even a long time after mild irradiation.

4.4. Glial cells and ECS diffusion parameters during demyelinating diseases

Experimental autoimmune encephalomyelitis (EAE) is widely used as an animal model for the human inflammatory demyelinating disease, multiple sclerosis (for review see Lassmann, 1983; Lassmann et al., 1986). In experiments in which EAE was induced by an injection of guinea-pig myelin basic protein, typical morphological changes in the CNS tissue could be observed including demyelination, inflammatory reaction, astrogliosis, blood–brain barrier damage as well as paralysis at 14–17 days post-injection (Šimonová et al., 1996). EAE was accompanied by increases in the ECS volume fraction in all regions of the spinal cord (Fig. 5C), namely in the dorsal horn (from 0.21 to 0.28), the ventral horn (from 0.23 to 0.47), the intermediate region (from 0.22 to 0.33) and in white matter (from 0.18 to 0.30). A significant decrease in tortuosity was observed in the dorsal horn and in the intermediate region and a decrease in nonspecific uptake in the intermediate region and in the ventral horn. There was a close correlation between the changes in ECS diffusion parameters and the manifestation of neurological abnormalities (paraparesis, paraplegia), which were preceded and greatly outlasted by the astrogliosis and inflammatory reaction.

These results indicate that an increase in the ECS volume may also alter the diffusion parameters of nervous tissue during inflammatory and demyelinating diseases, and may thus decrease the efficacy of synaptic as well as non-synaptic transmission and intercellular communication during these disorders.

4.5. Glial cells and ECS diffusion parameters in grafted tissue

In experiments in which embryonic cortical or tectal tissue was transplanted onto the dorsal surface of the midbrain of neonatal rats, astrogliosis and the formation of myelinated tracts were observed (Harvey et al., 1997; Syková et al., 1999b). Grafted tissue matured in the host brain and developed characteristic cytoarchitectural features. In both types of graft, astrocytes were hypertrophied, stained intensely for GFAP, and remained in a reactive state for many months after transplantation, while oligodendrocytes matured in an apparently normal manner in both tectal and cortical transplants and attained relatively normal phenotypic characteristics (Harvey et al., 1993, 1997). In the study of Syková et al. (1999b) comparisons were made between the diffusion parameters of host cortex and corpus callosum, fetal cortical or tectal tissue transplanted to host midbrain and fetal cortical tissue transplanted to host cortex (“cortex-to-cortex”). In host cortex, volume fraction ranged from 0.20 to 0.21 and tortuosity from 1.59 to 1.64, while in cortical as well as tectal grafts, 81–150 days post-transplantation, much higher values were observed: volume fraction ranged from 0.29 to 0.34 and tortuosity from 1.78 to 1.85 (Fig. 5D). Further analysis revealed that diffusion in grafts was anisotropic and more hindered than in host cortex. The heterogeneity of diffusion parameters correlated with the structural heterogeneity of the neuropil, with the highest values of volume fraction in gray matter and the highest values of tortuosity in white matter bundles. In “old” cortical grafts (one year post-transplantation) the values of volume fraction and tortuosity were significantly lower than in “young” grafts, and a clear decrease in GFAP immunoreactivity throughout the grafted tissue was observed. In cortex-to-cortex grafts, ECS volume fraction and tortuosity varied with the degree of graft incorporation into host tissue and with the degree of astrogliosis, but on average they were significantly lower than in young cortical and tectal grafts. Well-incorporated grafts revealed relatively less astrogliosis, and the values of ECS diffusion parameters were not significantly higher than those in normal host cortex.

The observed changes of ECS diffusion parameters in transplanted tissue could affect the movement and accumulation of neuroactive substances and thus impact neuron-glia communication and synaptic and extrasynaptic transmission in the grafts, and may thus have potential relevance to human neuropathological conditions associated with acute or chronic astrogliosis.

5. Diffusion properties of the nervous tissue during aging

Aging, Alzheimer’s disease and many degenerative diseases are accompanied by various pathological processes including a decreased number and efficacy of synapses, a decrease in transmitter release, neuronal loss, astrogliosis, demyelination, deposits of beta amyloid, changes in extracellular matrix proteins, etc. In our recent study in the rat brain, morphological changes during aging included cell loss, loss of dendritic processes, demyelination, astrogliosis, swollen astrocytic processes and changes in the extracellular matrix. Increased GFAP staining and an increase in the size and fibrous character of astrocytes were found in the cortex, corpus callosum and hippocampus of senescent

rats, which may account for changes in the ECS volume fraction (Syková et al., 1998a).

The ECS diffusion parameters were measured in the cortex, corpus callosum and hippocampus (CA1, CA3 and dentate gyrus). TMA^+ diffusion was measured in the ECS independently along three orthogonal axes (x — transversal, y — sagital, z — vertical). In all three regions — cortex, corpus callosum and hippocampus — the mean ECS volume fraction α was significantly lower in aged rats (26–32 months old), ranging from 0.16 to 0.18, than in young adults (3–4 months old) in which α ranged from 0.21 to 0.22 (Fig. 6). Nonspecific uptake k' was also significantly lower in aged rats.

Morphological changes other than those accounting for the α decrease could account for the decreases in λ values and for the disruption of tissue anisotropy. In the hippocampus in CA1, CA3, as well as in the dentate gyrus, we observed changes in the arrangement of fine astrocytic processes. These are normally organized in parallel in the x–y plane, and this organization totally disappears during aging. Moreover, the decreased staining for chondroitin sulfate proteoglycans and for fibronectin suggests a loss of extracellular matrix macromolecules. Although the mean tortuosity values along the x-axis were not significantly different between young and aged rats, the values were significantly lower in aged rats along the y- and z-axes, and thus the values along all three axes become almost the same (Fig. 6). This means that there is a loss of anisotropy in the aging hippocampus, particularly in the CA3 region and the dentate gyrus (Syková et al., 1998a).

The observed loss of anisotropy in senescent rats could therefore lead to impaired cortical and, particularly, hippocampal function. The decrease in ECS size could be responsible for the greater susceptibility of the aged brain to pathological events, particularly ischemia (Syková et al., 1998a), the poorer outcome of clinical therapy and the more limited recovery of affected tissue after insult.

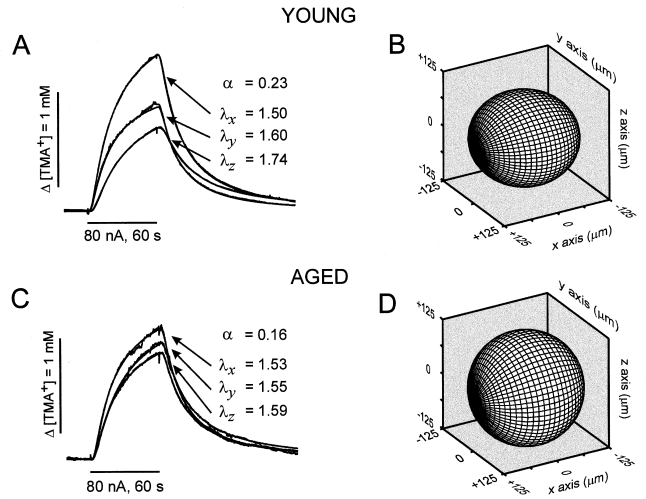

Fig. 6. Diffusion parameters in the hippocampus dentate gyrus of a young adult and an aged rat. A: Anisotropic diffusion in the dentate gyrus of a young adult rat. TMA^+ diffusion curves (concentration-time profiles) were measured along three orthogonal axes (x — mediolateral, y — rostrocaudal, z — dorsoventral). The slower rise in the z than in the y direction and in the y than in the x direction indicates a higher tortuosity and more restricted diffusion. The amplitude of the curves shows that TMA^+ concentration is much higher along the x-axis than along the y-axis and z-axis (λ_x, λ_y, λ_z). Actual ECS volume fraction α is about 0.2 and can be calculated only when measurements are done along the x-, y- and z-axes. B: Iso-concentration surfaces for a 0.1 mM TMA^+ concentration contour 60 s after the onset of a 80 nA iontophoretic pulse. The surfaces were generated using mean values of volume fraction and tortuosity. Anisotropic diffusion in a young adult rat is represented by the ellipsoid. C: In an aged rat diffusion curves are higher, showing that α is smaller and anisotropy is almost lost. D: The larger sphere in an aged rat, corresponding to isotropic diffusion and to a lower ECS volume fraction, demonstrates that diffusion from any given source will lead to a higher concentration of substances in the surrounding tissue and a larger action radius in aged rats than in young adults.

6. Are glial membrane properties affected by regional differences in ECS volume?

It was shown in recent studies that the regional differences in extracellular space volume around glial cells in the CNS affect their membrane currents in response to voltage steps (Berger et al., 1991; Chvátal et al., 1997, 1999). Glial cells are almost exclusively permeable for K^+, thus depolarization of the glial membrane causes a massive efflux of K^+ out of the cell. It was shown using the patch-clamp technique that in cultured oligodendrocytes, the current evoked by the depolarization exactly matched the shape of the depolarizing pulse (Sontheimer and Kettenmann, 1988; Sontheimer et al., 1989). In contrast, depolarization of oligodendrocytes in the white matter of brain slices, where the ECS is more compact in comparison to the almost infinite ECS in cell culture, evoked decaying currents during the cell depolarization and large tail currents after the offset of the voltage command (Berger et al., 1991; Chvátal et al., 1997). The reversal potential of the cell shifted after the voltage jump and the time constant of the observed current decay was independent of the voltage, but varied from cell to cell. Moreover, the reversal potential of the tail currents was dependent on the duration and amplitude of the voltage command, and thus it was possible to conclude that the current decay as well as the tail currents observed in oligodendrocytes were caused by a marked K^+ accumulation in the vicinity of the cell membrane, due to a change in the potassium equilibrium potential. These results were confirmed in experiments in which the membrane properties of cells of the oligodendrocyte lineage were compared with the ECS diffu-

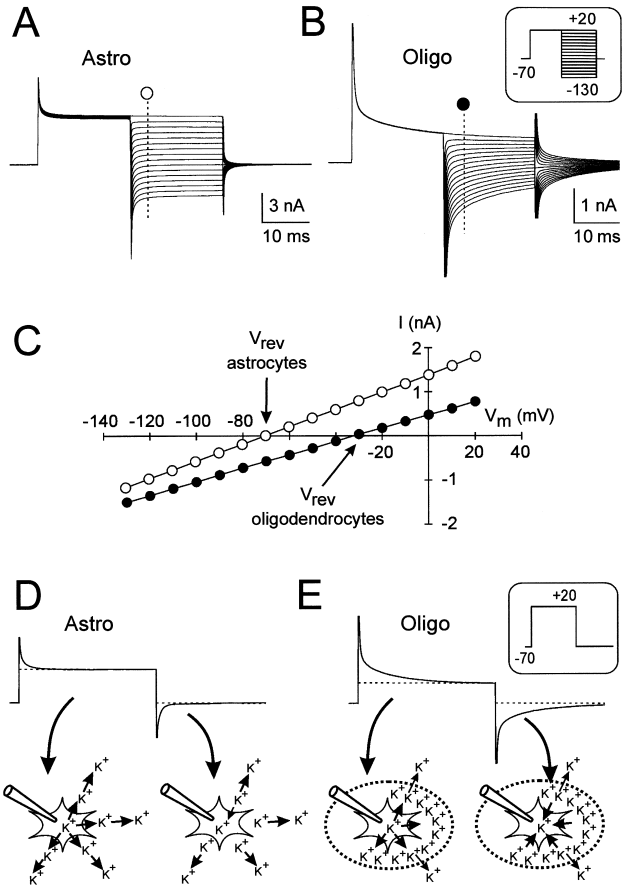

Fig. 7. Membrane properties and tail current analysis in astrocytes and oligodendrocytes and a scheme for a hypothesis of K^+ movements across astrocytic and oligodendrocytic membrane. A, B: For the tail current analysis the membranes of astrocytes and oligodendrocytes were clamped from a holding potential of −70 mV to +20 mV for 20 ms. After this prepulse, the membrane was clamped for 20 ms to increasing de- and hyperpolarizing potentials (pattern of voltage commands in inset) ranging from −130 mV to +20 mV, at 10 mV increments. The corresponding current traces are superimposed. C: From traces as shown in astrocytes (A) and oligodendrocytes (B) currents (I) were measured 5 ms after the onset of the de- and hyperpolarizing pulses (dashed lines) and plotted as a function of the membrane potential (V_m). The reversal potentials (V_{rev}) are indicated in the graphs by the arrows. In the oligodendrocytes, in contrast to the astrocytes, the depolarizing prepulse shifted the reversal potential from about −70 mV to about −31 mV. D, E: Hypothesis of the K^+ shift across astrocytic and oligodendrocytic membranes during and after the depolarizing pulse on a cellular level. During the depolarizing pulse, K^+ is extruded from the cell to the extracellular space. In astrocytes (D), extruded K^+ freely moves away from the membrane, so within several milliseconds a steady-state is established, i.e. the majority of K^+ that is leaving the cell is freely redistributed in the ECS. After the offset of the voltage command, only a small amount of K^+ re-enters the cell, creating a very small tail current. In oligodendrocytes (E), presumed diffusion barriers (dashed ellipse) prevent K^+ from moving freely away and thus K^+ accumulates in the vicinity of the cell membrane. During this accumulation, a new K^+ equilibrium is established, which is reflected by the decreasing current during the voltage step. After the offset of the depolarizing prepulse, K^+ moves back to the cell and produces prominent tail currents.

sion parameters of rat corpus callosum during development from postnatal day 10 to 20 (P10–P20), i.e., during the period of extensive myelination. At P10, when the majority of cells in the white matter are glial precursors, no tail currents were measured in these cells and the ECS volume fraction was $\alpha = 0.36$. In contrast, in white matter after myelination at P20, characterized by the presence of mature oligodendrocytes with decaying currents and large tail currents after the offset of a voltage jump, the ECS volume fraction was significantly smaller, $\alpha = 0.25$.

In experiments performed in the gray matter of the spinal cord slice, i.e. in tissue containing neurons as well as mature astrocytes and oligodendrocytes and their respective precursors (Chvátal et al., 1995), the occurrence of large tail currents was observed only in oligodendrocytes but not in other cell types (Fig. 7; Chvátal et al., 1999). As calculated from the Nernst equation, changes in the reversal potentials of the tail currents revealed a significantly larger accumulation of $[K^+]_e$ around oligodendrocytes than around astrocytes during the depolarization of the cells, apparently due to the more "compact" ECS around oligodendrocytes (Fig. 7D, E). The application of 50 mM K^+ or hypotonic solution, used to study the effect of cell swelling on the changes in $[K^+]_e$ evoked by a depolarizing pulse, produced in vicinity of astrocytes an increase in $[K^+]_e$ in the range of 200–240%, while in oligodendrocytes such an increase was only 22–30%.

ECS diffusion measurements in nervous tissue, which are performed by means of the real-time iontophoretic method over a volume on the order of 10^{-3} mm^3, do not provide information about the properties of the ECS in the vicinity of individual nerve cells. Nevertheless, using tail current analysis to study the glial membrane properties it became evident that the larger K^+ accumulation in the vicinity of the oligodendrocyte membrane results from a smaller ECS volume around oligodendrocytes than around astrocytes. These results also indicate that the swelling is more pronounced in astrocytes than in oligodendrocytes, and it is possible to speculate that astrocytes are responsible for the majority of the cell volume changes in nervous tissue. In addition, the electrophysiological properties of oligodendrocytes, i.e., the K^+ influx indicated by the presence of tail currents, shows that this type of cell may efficiently contribute to the regulation of K^+ changes arising from neuronal activity.

7. Conclusions

We conclude that glial cells control not only ECS ionic composition, but also ECS size and geometry. Since the ECS ionic and volume changes have been shown to play an important role in modulating the

complex synaptic and nonsynaptic signal transmission in the CNS, glial cells may thus affect neuronal interaction and synchronization and neuron–glia communication. As shown in Fig. 3 a link between ionic and volume changes and signal transmission has been proposed in a model of a non-specific feedback mechanism suppressing neuronal activity (Syková, 1997). First, neuronal activity results in the accumulation of $[K^+]_e$, which in turn depolarizes glial cells, and this depolarization induces an alkaline shift in glial pH_I. Second, the glial cells extrude acid and the resulting acid shift causes a decrease in the neuronal excitability. Because the ionic transmembrane shifts are always accompanied by water, this feedback mechanism is amplified by activity-related glial swelling compensated for by ECS volume shrinkage and by increased tortuosity, presumably by the crowding of molecules of the ECS matrix and/or by the swelling of fine glial processes. This, in turn, results in a larger accumulation of ions and other neuroactive substances in the brain due to more hindered diffusion in the ECS.

Astrocyte hypertrophy, proliferation and swelling can influence not only the size of the ECS volume but also the ECS tortuosity around neurons, slowing down diffusion in the ECS and thus modulating neuronal activity and neuron-glia interaction. This can affect diffusion anisotropy, which could be an underlying mechanism for the specificity of extrasynaptic transmission. Several recent studies, for instance, suggest the occurrence of a "spillover" of glutamate or GABA and "cross-talk" between distinct synapses (Barbour and Hausser, 1997; Kullmann and Asztely, 1998). An increased concentration of transmitter released into a synapse (e.g. repetitive adequate stimuli or during high frequency electrical stimulation which induces LTP) results in a significant activation of high-affinity receptors at neighboring synapses. The efficacy of such synaptic cross-talk would be dependent on the extracellular space surrounding the synapses, i.e., on intersynaptic geometry and diffusion parameters. Other recent studies also suggested an important role for proteoglycans, known to participate in multiple cellular processes such as axonal outgrowth, axonal branching and synaptogenesis (Hardington and Fosang, 1992; Margolis and Margolis, 1993) that are important for the formation of memory traces. Recently we observed an increased tortuosity in isolated rat spinal cord after the application of hyaluronic acid into the bathing solution (Prokopová et al., 1996). Moreover, we found a decrease of fibronectin and chondroitin-sulphate proteoglycan staining in the hippocampus of mildly behaviorally impaired aged rats and almost a complete loss of staining in severely impaired aged rats (Syková et al., 1998a, b). It is therefore reasonable to assume that besides neuronal and glial processes the macromolecules of the extracellular matrix contribute to the diffusion barriers in the ECS.

It is apparent that glial cells play an important role in ionic and volume homeostasis during physiological as well as pathological states. Affecting the local architecture of the CNS, they may be also involved in the modulation of signal transmission, in plastic changes such as long-term potentiation or depression, and in changes of behavior and memory formation.

Acknowledgements

Supported by grants VS 96-130, GA ČR 307/96/K226, GA ČR 309/97/K048, GA ČR 309/99/0657 and GA ČR 305/99/0655.

References

Agnati, L.F., Zoli, M., Strömberg, I., Fuxe, K., 1995. Intercellular communication in the brain: wiring versus volume transmission. Neuroscience 69, 711–726.

Andrew, R.D., MacVicar, B.A., 1994. Imaging cell volume changes and neuronal excitation in the hippocampal slice. Neuroscience 62, 371–383.

Barbour, B., Hausser, M., 1997. Intersynaptic diffusion of neurotransmitter. Trends in Neurosciences 20, 377–384.

Benveniste, H., Hedlund, L.W., Johnson, G.A., 1992. Mechanism of detection of acute cerebral ischemia in rats by diffusion-weighted magnetic resonance microscopy. Stroke 23, 746–754.

Berger, T., Schnitzer, J., Kettenmann, H., 1991. Developmental changes in the membrane current pattern, K^+ buffer capacity and morphology of glial cells in the corpus callosum slice. Journal of Neuroscience 11, 3008–3024.

Chesler, M., 1990. The regulation and modulation of pH in the nervous system. Progress in Neurobiology 34, 401–427.

Chvátal, A., Anděrová, M., Žiak, D., Syková, E., 1999. Glial depolarization evokes a larger potassium accumulation around oligodendrocytes than around astrocytes in gray matter of rat spinal cord slices. Journal of Neuroscience Research 56, 493–505.

Chvátal, A., Berger, T., Voříšek, I., Orkand, R.K., Kettenmann, H., Syková, E., 1997. Changes in glial K^+ currents with decreased extracellular volume in developing rat white matter. Journal of Neuroscience Research 49, 98–106.

Chvátal, A., Pastor, A., Mauch, M., Syková, E., Kettenmann, H., 1995. Distinct populations of identified glial cells in the developing rat spinal cord: ion channel properties and cell morphology. European Journal of Neuroscience 7, 129–142.

Cserr, H.F., De Pasquale, M., Nicholson, C., Patlak, C., Pettigrew, K.D., Rice, M.E., 1991. Extracellular volume decreases while cell volume is maintained by ion uptake in rat brain during acute hypernatremia. Journal of Physiology (London) 442, 277–295.

Deitmer, J.W., Rose, C.R., 1996. pH regulation and proton signalling by glial cells. Progress in Neurobiology 48, 73–103.

Fike, J.R., Gobbel, G.T., 1991. Central nervous system radiation injury in large animal models. In: Gutin, P.H., Leibel, S.A., Sheline, G.E. (Eds.), Radiation Injury to the Nervous System. Raven Press, New York, pp. 113–135.

Gilmore, S.A., 1964. The effects of X-irradiation on the spinal cords of neonatal rats. II. Histological observations. Journal of Neuropathology and Experimental Neurology 22, 294–301.

Gullans, S.R., Verbalis, J.G., 1993. Control of brain volume during

hyperosmolar and hypoosmolar conditions. Annual Review of Medicine 44, 289–301.

Hardington, T.E., Fosang, A.J., 1992. Proteoglycans: many forms and many functions. FASEB Journal 6, 861–870.

Harvey, A.R., Kendall, C.L., Syková, E., 1997. The status and organization of astrocytes, oligodendroglia and microglia in grafts of fetal rat cerebral cortex. Neuroscience Letters 227, 58–62.

Harvey, A.R., Plant, G.W., Kent, A.P., 1993. The distribution of astrocytes, oligodendroglia and myelin in normal and transplanted rat superior colliculus: an immunohistochemical study. Journal of Neural Transplant Plasticity 4, 1–14.

Hatten, M.E., Liem, R.K.H., Shelanski, M.L., Mason, C.A., 1991. Astroglia in CNS injury. Glia 4, 233–243.

Heinemann, U., Lux, H.D., 1977. Ceiling of stimulus-induced rises of extracellular potassium concentration in the cerebral cortex of the cat. Brain Research 120, 231–249.

Jendelová, P., Syková, E., 1991. Role of glia in K^+ and pH homeostasis in the neonatal rat spinal cord. Glia 4, 56–63.

Jendelová, P., Chvátal, A., Šimonová, Z., Syková, E., 1994. Effect of excitatory amino acids on extracellular pH in isolated rat spinal cord. In: Abstracts of the Seventeenth Annual Meeting of ENA, Vienna, p. 199.

Kimelberg, H.K., 1991. Swelling and volume control in brain astroglial cells. In: Gilles, R., et al. (Eds.), Advances in Comparative and Environmental Physiology. Springer-Verlag, Berlin, Heidelberg, pp. 81–117.

Kimelberg, H.K., Ransom, B.R., 1986. Physiological and pathological aspects of astrocyte swelling. In: Federoff, S., Vernadakis, A. (Eds.), Astrocytes: Cell Biology and Pathology of Astrocytes. Academic Press, New York, pp. 129–166.

Kimelberg, H.K., Sankar, P., O'Connor, E.R., Jalonen, T., Goderie, S.K., 1992. Functional consequences of astrocyte swelling. Progress in Brain Research 94, 57–68.

Korf, J., Klein, H.C., Postrema, F., 1988. Increases in striatal and hippocampal impedance and extracellular levels of amino acids by cardiac arrest in freely moving rats. Journal of Neurochemistry 50, 1087–1096.

Križaj, D., Rice, M.E., Wardle, R.A., Nicholson, C., 1996. Water compartmentalization and extracellular tortuosity after osmotic changes in cerebellum of *Trachemys scripta*. Journal of Physiology (London) 492, 887–896.

Kříž, N., Syková, E., Vyklický, L., 1975. Extracellular potassium changes in the spinal cord of the cat and their relation to slow potentials, active transport and impulse activity. Journal of Physiology (London) 249, 167–182.

Kullmann, D.M., Asztely, F., 1998. Extrasynaptic glutamate spillover in the hippocampus: evidence and implications. Trends in Neurosciences 21, 8–14.

Lassmann, H., 1983. Comparative Neuropathology of Chronic Experimental Allergic Encaphalomyelitis and Multiple Sclerosis. Springer, Berlin.

Lassmann, H., Vass, K., Brunner, Ch, Seitelberger, F., 1986. Characterization of inflammatory infiltrates in experimental allergic encaphalomyelitis. Progress in Neuropathology 6, 33–62.

Latour, L.L., Svoboda, K., Mitra, P.P., Sotak, C.H., 1994. Time-dependent diffusion of water in a biological model system. Proceedings of the National Academy of Sciences of the USA 91, 1229–1233.

Lehmenkühler, A., Syková, E., Svoboda, J., Zilles, K., Nicholson, C., 1993. Extracellular space parameters in the rat neocortex and subcortical white matter during postnatal development determined by diffusion analysis. Neuroscience 55, 339–351.

Margolis, R.K., Margolis, R.U., 1993. Nervous tissue proteoglycans. Experientia 49, 429–446.

Matsuoka, Y., Hossmann, K.A., 1982. Cortical impedance and extracellular volume changes following middle cerebral artery occlusion in cats. Journal of Cerebral Blood Flow and Metabolism 2, 466–474.

Mazel, T., Šimonová, Z., Syková, E., 1998. Diffusion heterogeneity and anisotropy in rat hippocampus. NeuroReport 9, 1299–1304.

Ng, K.T., Gibbs, M.E., Crowe, S.F., Sedman, G.L., Hua, F., Zhao, W., et al., 1992. Molecular mechanisms of memory formation. Molecular Neurobiology 5, 333–350.

Nicholson, C., 1995. Interaction between diffusion and Michaelis-Menten uptake of dopamine after iontophoresis in striatum. Biophysical Journal 68, 1699–1715.

Nicholson, C., Phillips, J.M., 1981. Ion diffusion modified by tortuosity and volume fraction in the extracellular microenvironment of the rat cerebellum. Journal of Physiology (London) 321, 225–257.

Nicholson, C., Syková, E., 1998. Extracellular space structure revealed by diffusion analysis. Trends in Neurosciences 21, 207–215.

Nicholson, C., Tao, L., 1993. Hindered diffusion of high molecular weight compounds in brain extracellular microenvironment measured with integrative optical imaging. Biophysical Journal 65, 2277–2290.

Norris, D.G., Niendorf, T., Leibfritz, D., 1994. Healthy and infarcted brain tissues studied at short diffusion times: the origins of apparent restriction and the reduction in apparent diffusion coefficient. NMR in Biomedicine 7, 304–310.

Norton, W.T., Aquino, D.A., Hosumi, I., Chiu, F.C., Brosnan, C.F., 1992. Quantitative aspects of reactive gliosis: a review. Neurochemical Research 17, 877–885.

Pérez-Pinzon, M.A., Tao, L., Nicholson, C., 1995. Extracellular potassium, volume fraction, and tortuosity in rat hippocampal CA1, CA3 and cortical slices during ischemia. Journal of Neurophysiology 74, 565–573.

Prokopová, Š, Nicholson, C., Syková, E., 1996. The effect of 40-kDa or 70-kDa dextran and hyaluronic acid solution on extracelluar space tortuosity in isolated rat spinal cord. Physiological Research 45, P28.

Prokopová, Š, Vargová, L., Syková, E., 1997. Heterogeneous and anisotropic diffusion in the developing rat spinal cord. NeuroReport 8, 3527–3532.

Rice, M.E., Okada, Y., Nicholson, C., 1993. Anisotropic and heterogeneous diffusion in the turtle cerebellum. Journal of Neurophysiology 70, 2035–2044.

Ridet, J.I., Malhotra, S.K., Privat, A., Gage, F.H., 1997. Reactive astrocytes: cellular and molecular cues to biological function. Trends in Neurosciences 20, 570–577.

Roitbak, T., Syková, E., 1999. Diffusion barriers evoked in the rat cortex by reactive astrogliosis. Glia 20, 40–48.

Šimonová, Z., Svoboda, J., Orkand, P., Bernard, C.C.A., Lassmann, H., Syková, E., 1996. Changes of extracellular space volume and tortuosity in the spinal cord of Lewis rats with experimental autoimmune encephalomyelitis. Physiological Research 45, 11–22.

Sims, T.J., Gilmore, S.A., 1992. Glial response to dorsal root lesion in the X-irradiated spinal cord. Glia 6, 96–107.

Sontheimer, H., Kettenmann, H., 1988. Heterogeneity of potassium currents in cultured oligodendrocytes. Glia 1, 415–420.

Sontheimer, H., Trotter, J., Schachner, M., Kettenmann, H., 1989. Channel expression correlates with differentiation stage during the development of oligodendrocytes from their precursor cells in culture. Neuron 2, 1135–1145.

Strange, K., 1992. Regulation of solute and water balance and cell volume in the central nervous system. Journal of the American Society for Nephrology 3, 12–27.

Syková, E., 1983. Extracellular K^+ accumulation in the central nervous system. Progress in Biophysics and Molecular Biology 42, 135–189.

Syková, E., 1992. Ionic and volume changes in the microenviron-

ment of nerve and receptor cells. In: Ottoson, D. (Ed.), Progress in Sensory Physiology. Springer-Verlag, Heidelberg, pp. 1–167.

Syková, E., 1997. The extracellular space in the CNS: Its regulation, volume and geometry in normal and pathological neuronal function. The Neuroscientist 3, 28–41.

Syková, E., Jendelová, P., Šimonová, Z. Chvátal A., 1992. K^+ and pH homeostasis in the developing rat spinal cord is impaired by early postnatal X-irradiation. Brain Research 594, 19–30.

Syková, E., Mazel, T., Šimonová, Z., 1998a. Diffusion constraints and neuron-glia interaction during aging. Experimental Gerontology 33, 837–851.

Syková, E., Mazel, T., Frisch, C., Šimonová, Z., Hasenöhrl, R.U., Huston, J.P., 1998b. Spatial memory and diffusion parameters in aged rat cortex, corpus callosum and hippocampus. Society for Neuroscience Abstracts 24 (1), 1420.

Syková, E., Rothenberg, S., Krekule, I., 1974. Changes of extracellular potassium concentration during spontaneous activity in the mesencephalic reticular formation of the rat. Brain Research 79, 333–337.

Syková, E., Svoboda, J., 1990. Extracellular alkaline-acid-alkaline transients in the rat spinal cord evoked by peripheral stimulation. Brain Research 512, 181–189.

Syková, E., Svoboda, J., Šimonová, Z., Lehmenkühler, A., Lassmann, H., 1996. X-irradiation-induced changes in the diffusion parameters of the developing rat brain. Neuroscience 70, 597–612.

Syková, E., Mazel, T., Roitbak, T., Šimonová, Z., 1999a. Morphological changes and diffusion barriers in auditory cortex and hippocampus of aged rats. Association for Research in Otolaryngology Abstracts 22, 117.

Syková, E., Roitbak, T., Mazel, T., Šimonová, Z., Harvey, A.R., 1999b. Astrocytes, oligodendroglia, extracellular space volume and geometry in rat fetal brain grafts. Neuroscience 91, 783–798.

Syková, E., Vargová, L., Prokopová, Š, Šimonová, Z., 1999c. Glial swelling and astrogliosis produce diffusion barriers in the rat spinal cord. Glia 25, 56–70.

Van der Toorn, A., Syková, E., Dijkhuizen, R.M., Vořišek, I., Vargová, L., Škobisová, E., Van Lookeren Campagne, M., Reese, T., Nicolay, K., 1996. Dynamic changes in water ADC, energy metabolism, extracellular space volume, and tortuosity in neonatal rat brain during global ischemia. Magnetic Resonance in Medicine 36, 52–60.

Van Harreveld, A., Dafny, N., Khattab, F.I., 1971. Effects of calcium on electrical resistance and the extracellular space of cerebral cortex. Experimental Neurology 31, 358–367.

Vořišek, I., Syková, E., 1997. Evolution of anisotropic diffusion in the developing rat corpus callosum. Journal of Neurophysiology 78, 912–919.

Walker Jr, J.L., 1971. Ion specific liquid ion exchanger microelectrodes. Analytical Chemistry 43, 89A–93A.

Zoli, M., Jansson, A., Syková, E., Agnati, L.F., Fuxe, K., 1999. Intercellular communication in the central nervous system. The emergence of the volume transmission concept and its relevance for neuropsychopharmacology. Trends in Pharmacological Sciences 20, 142–150.